

EFFECT OF LEAF ANATOMY ON HYPOSTOMATOUS LEAF GAS EXCHANGE : A THEORETICAL STUDY WITH THE 2DLEAF MODEL

Pachepsky, L. B.
USDA ARS Remote Sensing and Modeling Laboratory

Acock, B.
Duke University Department of Botany

<https://hdl.handle.net/2324/8236>

出版情報 : BIOTRONICS. 27, pp.1-14, 1998-12. Biotron Institute, Kyushu University
バージョン :
権利関係 :

EFFECT OF LEAF ANATOMY ON HYPOSTOMATOUS LEAF GAS EXCHANGE: A THEORETICAL STUDY WITH THE 2DLEAF MODEL

L. B. PACHEPSKY^{1,2} and B. ACOCK²

¹*Duke University, Department of Botany, Durham, NC 27708, USA*

²*USDA, ARS, Remote Sensing and Modeling Laboratory, Beltsville, MD 20705, USA*

(Received November 20, 1997; accepted March 23, 1998)

PACHEPSKY L. B. and ACOCK B. *Effect of leaf anatomy on hypostomatous leaf gas exchange: A theoretical study with the 2DLEAF model.* BIOTRONICS 27, 1–14, 1998. The two-dimensional model of leaf gas exchange, 2DLEAF, which accounts for leaf intercellular structure, was used to study the effect of leaf anatomy on the photosynthesis and transpiration rates of hypostomatous C₃ plants. The theoretical study was conducted to exclude the interacting effects of all other factors on leaf gas exchange; an exclusion that is very difficult to achieve in experiments with real leaves.

Clements (1905) identified four types of leaf anatomy, (1) staurophyll consisting entirely of palisade cells, (2) spongophyll containing only spongy cells, (3) diphotophyll composed of palisade cells adjacent to an adaxial and spongy cells adjacent to an abaxial sides of the leaf, and (4) diplophyll in which there are palisade cells adjacent to each leaf surface and spongy cells between them. These four types of leaf anatomy were studied assuming the same leaf thickness for all types and plus an additional thickness (+50%) for the diphotophyll.

Photosynthesis and transpiration rates calculated by 2DLEAF were compared for the same external conditions: 2000 $\mu\text{mol m}^{-2} \text{s}^{-1}$ (PPFD), 30°C, 60% relative air humidity, and 350 and 700 $\mu\text{mol m}^{-3}$ of CO₂ in air, [CO₂]. The biochemical parameters of 2DLEAF were given identical values for all anatomy types and both thicknesses. Stomatal density was assumed to be 300 per mm^{-2} and stomatal apertures were varied from 2 to 20 μm with an increment of 2 μm .

Photosynthesis rate at both values of [CO₂] depended on the internal leaf structure. For leaves of the same thickness, photosynthesis increased with increasing cell area index (CAI), the surface area of photosynthesizing cells per unit leaf surface area. Photosynthesis rate of a thick leaf of the same CAI value was lower than that of a thinner one, but this difference was less in high [CO₂]. Transpiration rates were less sensitive to changes in the internal leaf geometry than photosynthesis rates.

Key words: Leaf anatomy; hypostomatous plants; gas exchange; modeling.

Corresponding author: Ludmila Pachepsky Visiting Scientist RSML, ARS, USDA, Bldg 007, Rm 008, BARC-W 10300 Baltimore Ave Beltsville, MD 20705, USA

Tel : (301) 504-6042 Fax : (301) 504-5823 E-mail: lpachepsky@asrr.arsusda.gov

INTRODUCTION

Photosynthesis and transpiration are determined by different driving forces (CO₂ assimilation by mesophyll cells and water evaporation from their surfaces, respectively) yet they share a common domain for gas diffusion between the bulk atmosphere and mesophyll cell surfaces. For hypostomatous leaves, this domain consists of leaf intercellular space and a boundary layer. The thickness of the boundary layer depends on environmental conditions and on qualities of the leaf surface (17). The impact of the boundary layer on transpiration and photosynthesis has been examined experimentally and analyzed by models (22) although it is still quite a challenge to determine a thickness of boundary layer for a real leaf. Several approaches have been developed, both theoretical (e.g., 9) and empirical (e.g., 12). For the two-dimensional model of leaf gas exchange, 2DLEAF (19, 20), this parameter can be determined from transpiration data. Depending on the particular leaf properties there is a choice in 2DLEAF of varying either the boundary layer thickness or the value of the gas diffusion coefficient in the boundary layer.

Experimental data show that there is a significant effect of leaf intercellular geometry on the leaf gas exchange. Leaves of *Alocasia macrorrhiza* in 20% full sunlight in a greenhouse developed a total thickness 41% and a mesophyll thickness 52% greater than those grown in 1% full sunlight. The leaves did not change their type of structure as defined by Clements (2), but published leaf cross sections show that there was a difference in the internal leaf geometry. Maximum leaf photosynthetic capacity was also 60% greater for the high-light leaves (23). Dengler et al. (5) studied the leaf anatomy of 125 species of C₃ and C₄ grasses. Characteristics of mesophyll tissues were measured and their correlations with type of photosynthesis and assimilation pathways were established. In the work by Syvertsen *et al.* (24) internal conductances to CO₂ transfer for hypostomatous sun- and shade-grown leaves of three tree species were studied together with the anatomical characteristics of mesophyll tissues. Correlations of the internal conductance with the leaf thickness, the chloroplast surface area, and the fraction of intercellular air space in the mesophyll were found along with some other, more sophisticated, relationships. These results show that leaf anatomy seems to affect leaf gas exchange and that this effect can be analyzed quantitatively (24).

Leaf anatomy differs among species and within species under varying environmental conditions. Four types of leaf internal structure were described by Clements (2) after examining over 300 wild species from various habitats. Pronounced impacts of environmental factors, especially water and light, on the leaf anatomy of 24 species were reported. Similarly, Hanson (7) demonstrated an effect of light conditions on the proportion of palisade and spongy parenchyma in leaves of 6 tree species. Increased leaf thickness and changes in the number of palisade cell layers, density of cells, and cell sizes with simultaneous changes in photosynthesis were found for leaves of soybean, pine, and sweetgum grown in an atmosphere of elevated [CO₂] by Rogers *et al.* (21).

Changes in leaf photosynthesis in elevated $[\text{CO}_2]$ conditions are usually attributed to changes in assimilation rates and in leaf conductance (14, 15), but leaf conductance is a lumped parameter which is affected by both stomatal aperture and leaf geometry. In analyzing leaf photosynthesis, it seems desirable to separate changes in leaf anatomy from those of a biochemical nature and those caused by changes in stomatal aperture. This would increase the reliability of our predictions of plant response to $[\text{CO}_2]$ elevation.

Modeling is an efficient method of studying the effect of leaf anatomy on gas exchange. Natural variability in plants, leaves, tissues, enzymes, even within a species confounds the experimental isolation of the effect of leaf anatomy. Alternatively, numerical experiments with a validated model allow us to calculate leaf gas exchange for various leaf internal structures, keeping all other factors constant. The 2DLEAF model of leaf gas exchange, accounting for leaf anatomy, developed and validated for soybean and tomato (18, 19, 20) can be used to quantitatively study the pure effect of leaf anatomy on leaf gas exchange.

The objective of this study was to assess the importance of leaf anatomy for leaf photosynthesis and transpiration via simulations with the 2DLEAF model.

MATERIALS AND METHODS

To study the effects of leaf anatomy on photosynthesis and transpiration, we performed a series of numerical experiments with the two-dimensional model of leaf gas exchange, 2DLEAF, that explicitly accounts for leaf anatomy. Various leaf internal structures were evaluated, based on experimental data published by Clements (2).

2DLEAF

The model and parameter estimation techniques are described in detail elsewhere (19), so only a brief description is given here. The model describes two-dimensional flow of CO_2 , O_2 , and water vapor in the domain for hypostomatous leaves shown in Fig. 1b. The domain includes the leaf intercellular space, a substomatal cavity, half of a stomatal pore, and the boundary layer adjacent to the leaf. Cell surfaces also represent a part of the flow domain boundary as no gas flow occurs inside cells. These surfaces work as a source of water for evaporation, and relative air humidity on these surfaces is assumed to be 100%. For CO_2 assimilation, cell surfaces work as sinks for CO_2 . Gas concentrations on the outer border of the boundary layer are assumed to be equal to atmospheric concentrations. The three other borders of the flow domain cannot be crossed by gases. Two-dimensional gas diffusion occurs in the domain due to the concentration gradients. Fluxes through the stomate and internal gas concentrations are calculated. Flux of CO_2 through the stomate can be converted into the photosynthesis rate per unit of leaf area by multiplying an appropriate factor calculated from the data on stomatal density. Similarly the transpiration rate can be calculated from the water vapor flux through the

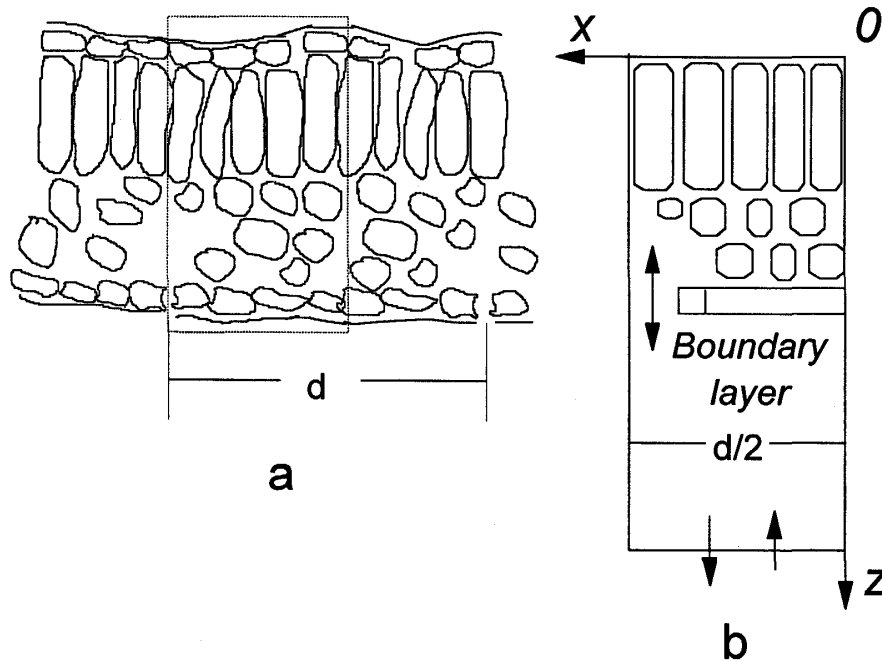


Fig. 1. Schematization of the leaf internal structure using (a) a leaf cross-section to construct (b) the domain for gas diffusion used in the 2DLEAF model. Dashed lines show the part of the cross-section presented at the domain and d —the distance between two stomates.

stomate.

The model is represented by (a) three equations of diffusion for the three gases, (b) six algebraic equations describing CO_2 assimilation on the cell surfaces which are in fact the boundary conditions for the CO_2 diffusion equation, (c) constant CO_2 , O_2 , and water vapor concentrations at the outer edge of the boundary layer which represent another part of the boundary conditions for the diffusion equations, and (d) temperature dependencies for some model parameters.

The diffusion equation is

$$\frac{\partial g}{\partial t} - D_g \frac{\partial^2 g}{\partial x^2} - D_g \frac{\partial^2 g}{\partial z^2} = 0$$

where g is the gas concentration (mol m^{-3}); x is a horizontal coordinate (m); z is a vertical coordinate (m) (Fig. 1); t is time (s); and D_g is the gas molecular diffusion coefficient in air ($\text{m}^2 \text{s}^{-1}$).

Assimilation of CO_2 is calculated for the surfaces of the palisade and spongy mesophyll cells. Carbon assimilation by cells is simulated as described by Farquhar *et al.* (6) and by Harley and Tenhunen (8). The rate of CO_2 assimilation per unit of cell surface, A , $\mu\text{mol m}^{-2} \text{s}^{-1}$, is described in the model as follows.

$$A = \left(1 - \frac{\Gamma}{C_j}\right) \min (W_c, W_j, W_p) - R_d;$$

$$W_c = \frac{V_{cmax} C_j}{C_j + K_c(1 + O/K_o)}; W_j = \frac{P_m}{1 + 2\Gamma/C_j}; W_p = 3 \frac{TPU}{1 - \Gamma/C};$$

$$P_m = \frac{\alpha I}{(1 + \alpha^2 I^2 / P_{lm}^2)^{0.5}}; R_d = b V_{cmax}$$

Here W_c is the Rubisco-limited rate of carboxylation, W_j and W_p are the RuBP-limited rates of carboxylation when RuBP regeneration is limited by electron transport and inorganic phosphate, respectively; R_d is respiration; all these variables are in $\mu\text{mol m}^{-2} \text{s}^{-1}$; Γ is the CO_2 compensation point in the absence of mitochondrial respiration, $\mu\text{L L}^{-1}$; V_{cmax} is the rate of RuBP carboxylation, $\mu\text{mol m}^{-2} \text{s}^{-1}$, C_j and O are internal concentrations of CO_2 and O_2 respectively, $\mu\text{L L}^{-1}$; K_c and K_o are Michaelis-Menten constants for carboxylation and oxygenation, respectively, $\mu\text{L L}^{-1}$; TPU is the rate of triose phosphate utilization, $\mu\text{mol m}^{-2} \text{s}^{-1}$; P_m , $\mu\text{mol m}^{-2} \text{s}^{-1}$, is the parameter introduced by Harley and Tenhunen (8) to describe a light dependency; I is incident photosynthetic photon flux density, $\mu\text{mol m}^{-2} \text{s}^{-1}$, α is the quantum use efficiency (on the incident-light basis) and P_{lm} is the rate of photosynthesis that occurs at CO_2 and light saturation, $\mu\text{mol m}^{-2} \text{s}^{-1}$. Water vapor pressure at the cell surfaces is set equal to the saturated value for the leaf temperature.

A procedure using a leaf cross-section (Fig. 1a), scanner and SigmaScan software is described in our earlier paper (19) for parameter estimation, leaf anatomy mapping and schematization (Fig. 1b). Temperature, air humidity, $[\text{CO}_2]$ in air, and light intensity are required to calculate transport and assimilation and to set the boundary conditions. The stomatal aperture can be calculated from environmental variables but for this particular study the stomatal aperture was an input variable with a range from 2 to 20 μm .

The 2DLEAF model contains 17 parameters. It was parameterized for tomato leaf in Pachevsky and Acock (19), and the same values given in Table 1 in that paper were used in the current study.

Variations in leaf anatomy

To study the effect of leaf anatomy on photosynthesis and transpiration we needed (1) a representative set of data on leaf anatomy and (2) a classification of leaf internal structures.

Clements (2) studied the leaf anatomy of more than 300 plants and presented leaf cross-sections of 61 wild species collected in the Colorado foothills and the Pike's Peak region of the Rocky mountains, USA. Both endemic and polidemic plants were examined. Four environmental factors were considered in conjunction with leaf structure, namely, light, soil water content, air humidity, and temperature. Measurements were taken during the summers of 1903 and 1904 with the means available at that time. Irradiation was measured by a

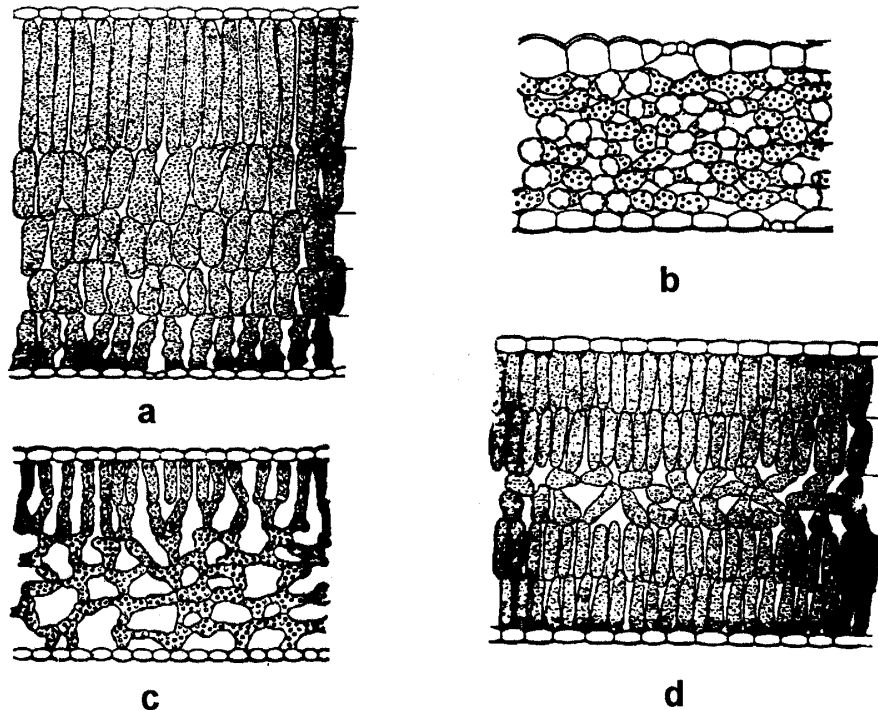


Fig. 2. Classification of leaf anatomy for endemic species according to Clements (1905) illustrated by (a) staurophyll *Bahia dissecta*, a xerophyte from mountain foothills, (b) spongophyll *Gyrostachys stricta*, a shade mesophyte from an open spruce forest, (c) diphotophyll *Arnica cordifolia*, a shade mesophyte from subalpine gravel, and (d) diplophyll *Touterea multiflora*, a sun xerophyte from subalpine gravel.

photometer, soil water content was determined by weighing. Automatic psychographs were used for continuous records of air humidity. During 15 weeks, continuous automatic records of temperature were made. Plants bearing mature leaves were gathered during flowering and/or fruit formation. Descriptions were based on the most typical part of the leaf cross-section.

Clements identified four types of leaf anatomy: (1) staurophyll, which is composed entirely of palisade cells (Fig. 2a), (2) spongophyll, which consists only of spongy mesophyll (Fig. 2b), (3) diphotophyll, which has palisade parenchyma adjacent to the upper epidermis and spongy tissue next to the lower epidermis (Fig. 2c), and (4) diplophyll, which has palisade parenchyma on both upper and lower sides of the leaf and spongy tissue between them (Fig. 2d).

We based the design of our numerical experiment on Clements' classification, i.e., staurophyll, spongophyll, diplophyll and four variations of diphotophylls (Fig. 3) were examined.

Parameters used in simulations with the 2DLEAF model

We chose a leaf thickness of 150 μm for these simulations because many wild plants and at least several agricultural plants, e.g., tomato, soybean, barley, and some cotton cultivars have leaf thicknesses close to this value (16, 27, 21,

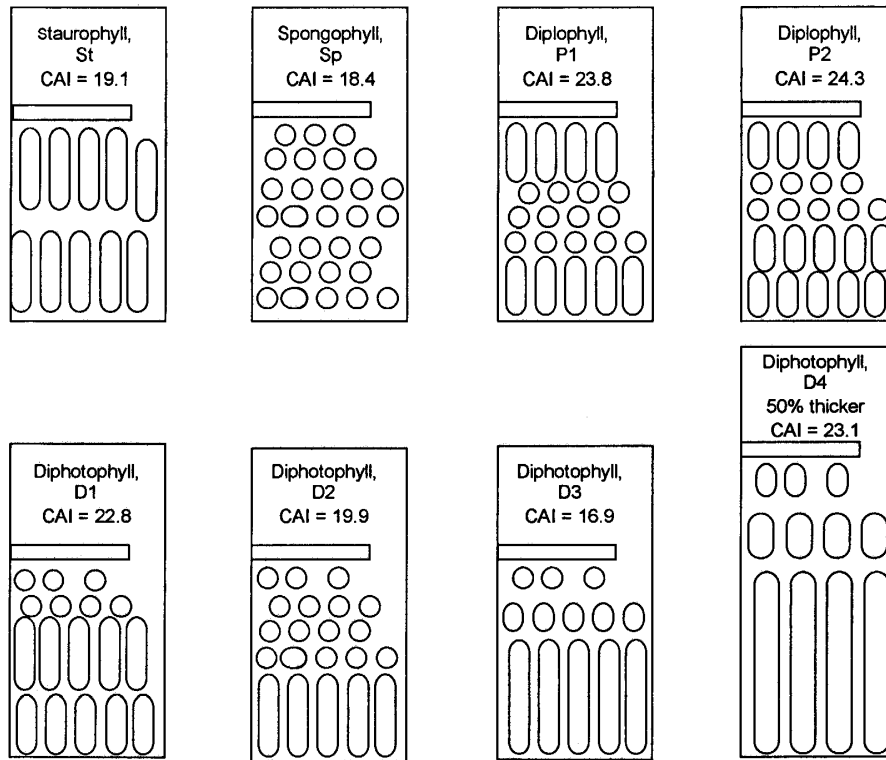


Fig. 3. Domains used in numerical experiments to calculate photosynthesis and transpiration for various types of leaf anatomy, cell area index, and leaf thickness. Stomatal density is assumed to be the same for all domains. Domain *g* (anatomy type D3) corresponds to a tomato leaf internal structure.

11). Cell sizes and stomatal densities for both palisade and spongy parenchyma were set equal to those for tomato plants. This information was used to calculate numbers and locations of cells for staurophyll and spongophyll leaves (Fig. 3, St and Sp).

For diplophyll and diphotophyll leaves (Fig. 3, P1 and P2) the numbers of palisade cell layers were set equal to 2 respectively as is often found in these types of leaves (2). Eighteen cross-sections of 45 polidemic diphotophyllic plants from various habitats had two layers of palisade cells, 20 of them had 3 palisade cell layers. In the variant presented in Fig. 3, D3 the palisade cells are 1.5 times as long as the variants in Fig. 3, St-D2, because endemic *Phacelia lyalii*, and polidemics *Pedicularis procer* and *Acer glabrum* had palisade cells about this size when found in well illuminated habitats (2).

A diphotophyllic leaf 50% thicker than the other leaves was examined to study the effect of leaf thickness. Not only does leaf thickness vary among species but variations in light (7, some trees) and $[CO_2]$ (21, soybean) can cause changes in leaf thickness within some species.

In this paper, we used a parameter, cell area index (CAI), the surface area of photosynthesizing cells per unit leaf surface area, to characterize the density of photosynthesizing cells. Values of CAI were different for the 8 leaf anatomies

designed for the current study (Fig. 3). The largest value of CAI was obtained for a cross-section with three layers of palisade mesophyll.

Driving variables

Calculations were made for all leaves using a PPFD of $2000 \mu\text{mol m}^{-2} \text{s}^{-1}$, leaf temperature 30°C , 60% relative air humidity, and two values of $[\text{CO}_2]$: 350 and $700 \mu\text{mol m}^{-3}$. Parameter values of the CO_2 assimilation submodel were computed using dependencies reported by Pachepsy and Acock (19) and held constant for all types of leaf anatomy. Stomatal aperture was an input variable ranging from 2 to $20 \mu\text{m}$. These environmental conditions and parameter values allowed us to examine only the effect of leaf anatomy on leaf photosynthesis and transpiration.

RESULTS

Results of simulating photosynthesis rates for eight leaf structures are presented in Fig. 4. There was a dependence of the photosynthesis rate on the internal leaf geometry at both, ambient (Fig. 4a) and doubled (Fig. 4b) CO_2 concentrations. The diplophyll leaf had the highest rate of photosynthesis at all stomatal aperture values (Fig. 4a) among all types of anatomy while the diplophyll with one palisade cell layer and two spongy cells layers had the

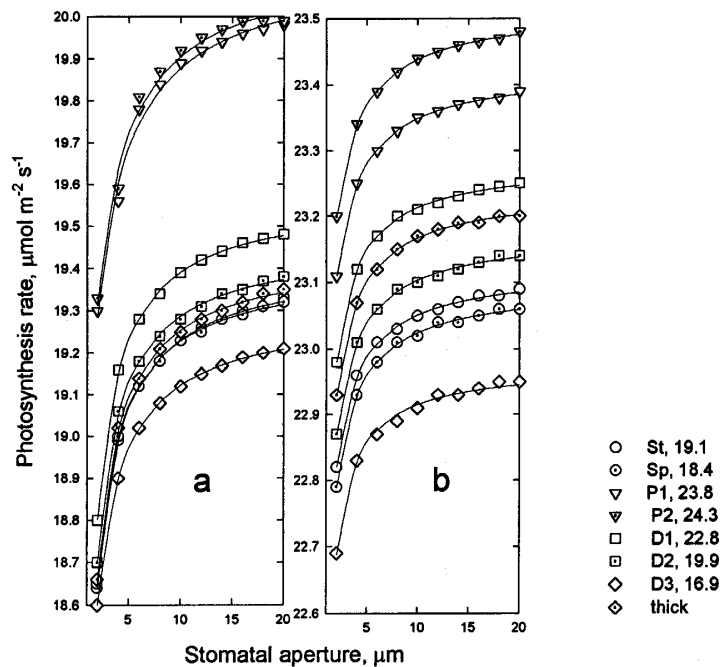


Fig. 4. Photosynthesis rates, $\mu\text{mol m}^{-2} \text{s}^{-1}$, at (a) 350 and (b) $700 \mu\text{mol m}^{-3}$ $[\text{CO}_2]$ for various leaf internal structures at PPFD of $2000 \mu\text{mol m}^{-2} \text{s}^{-1}$, 30°C , and 60% relative air humidity as functions of stomatal aperture, μm . Lines represent the approximations by formula (1). The codes for type of leaf anatomy are shown in Fig. 3 with the corresponding values of cell area index (CAI).

lowest rate of photosynthesis at both ambient and doubled $[\text{CO}_2]$, Fig. 4. The staurophyll and spongophyll structures had photosynthesis rates intermediate between those of the diplophyll with one palisade layer and the other diplophylls at both $[\text{CO}_2]$. The absolute values of the differences in photosynthesis rates were not very large, at the maximum, about 5% at ambient $[\text{CO}_2]$ and 2.5% at doubled $[\text{CO}_2]$. These differences were statistically significant.

When $[\text{CO}_2]$ was doubled, photosynthesis rate increased 17% for diplophyll and about 20% for all other types of leaf anatomy. The increase at higher $[\text{CO}_2]$ also was 1% greater for the staurophyll than for the spongophyll type of leaf anatomy (Fig. 4b).

Comparing Fig. 4a and Fig. 4b one can notice that differences in rate of photosynthesis were different at ambient and doubled $[\text{CO}_2]$. For example, at $350 \mu\text{mol m}^{-3} [\text{CO}_2]$ there was almost no difference in photosynthesis rate between staurophyll and diplophyll P1, between diplophyll D1 and spongophyll (Fig. 4a). The same differences at $700 \mu\text{mol m}^{-3} [\text{CO}_2]$ were much more pronounced, 5–10 fold increased.

The dependence of photosynthesis rate, y , $\mu\text{mol m}^{-2} \text{s}^{-1}$, on stomatal aperture, x , μm , can be described by the hyperbolic formula:

$$y = \frac{(a-c)x}{x+b} + c \quad (1)$$

where parameter a is the asymptotic rate of photosynthesis approached as x increases, the parameter c is the value of the photosynthesis rate approaches when $x = 0$, and parameter b defines the curvature. For all 16 curves presented in Fig. 4, parameter b values did not differ significantly from the mean value 0.455. Parameter c had different values for ambient and doubled CO_2 concentrations, but did not differ significantly within each of these groups from the mean value, 15.47– for ambient and 21.58– for doubled CO_2 concentrations. Values of parameter a (asymptote) were significantly different for all 16 curves. They are in a range between 19.29 and 20.07 for ambient, and from 22.98 to 23.51 for doubled CO_2 concentration. Therefore, the dependence of photosynthesis rate on stomatal aperture can be described with high precision (Fig. 4) by the formula

$$y = \frac{(a-15.47)x}{x+0.455} + 15.47$$

for ambient, and by the formula

$$y = \frac{(a-21.58)x}{x+0.455} + 21.58$$

for doubled CO_2 concentration.

Overall, the photosynthesis rate was proportional to CAI (Fig. 5), and this relationship was consistent for ambient and doubled $[\text{CO}_2]$.

The photosynthesis rate of a thick leaf was lower than that of a thin leaf with the same CAI value under all conditions (Fig. 5). The difference was less

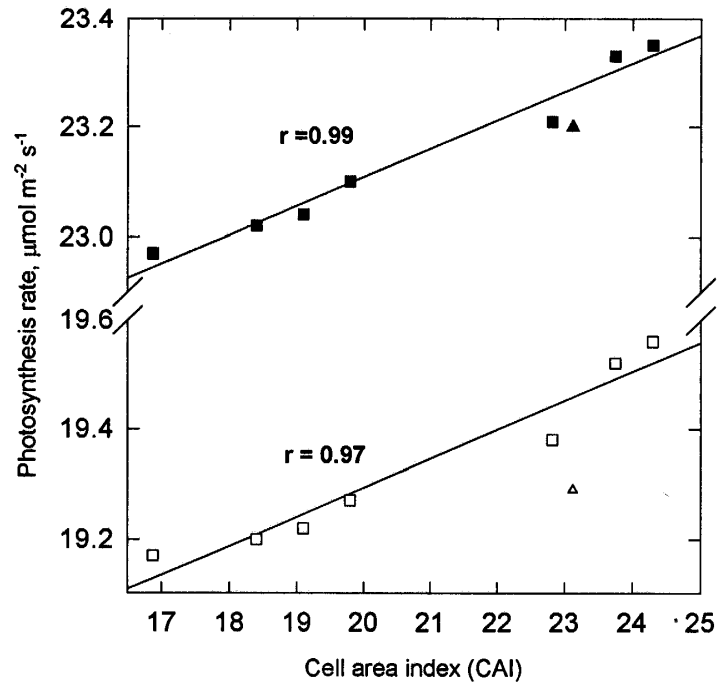


Fig. 5. Photosynthesis rate, $\mu\text{mol m}^{-2} \text{s}^{-1}$, at 350 (open squares) and 700 $\mu\text{mol m}^{-3}$ $[\text{CO}_2]$ (closed squares) as related to CAI. Triangle symbols (open for ambient and closed for double $[\text{CO}_2]$) show photosynthesis of a 50% thicker leaf of the D4 anatomy (Fig. 2).

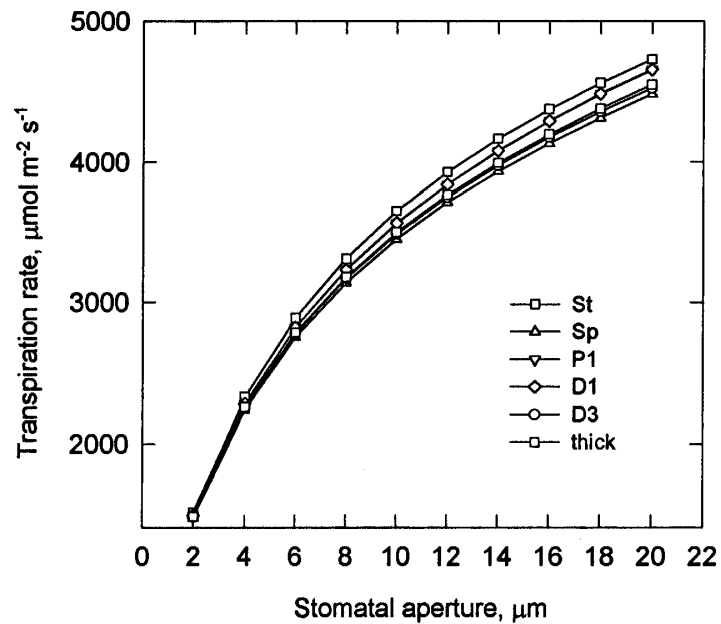


Fig. 6. Transpiration rates, $\mu\text{mol m}^{-2} \text{s}^{-1}$, for all leaf internal structures at 30°C and 60% relative air humidity as functions of stomatal aperture.

in doubled $[\text{CO}_2]$ than in an ambient $[\text{CO}_2]$.

Fig. 6 presents the results of the simulation of the transpiration rates for all leaf internal structures shown in Fig. 3. Differences were negligible, all within the range of the numerical method's accuracy.

DISCUSSION

Some plant species, like soybean (21), increase leaf thickness and the number of palisade layers when grow in an elevated $[\text{CO}_2]$ atmosphere. As a result, some additional sites of CO_2 assimilation arise and the leaf photosynthesis rate increases (26). Other species, like tomato, do not change their leaf internal structure in a changing environment (13, 16). Experimental data reported by Stanghellini and Bunce (25) did not show any difference in photosynthesis rate of tomato plants grown in ambient and elevated $[\text{CO}_2]$, when measured in the same environmental conditions. In future elevated $[\text{CO}_2]$ atmospheres, species with a flexible leaf anatomy may have advantages over other species. This could affect the choice of future crops and the process of breeding agricultural cultivars, as well as the composition of natural plant communities.

External factors which are predicted to vary in the course of global climate change, especially light and $[\text{CO}_2]$, may significantly change leaf anatomy (2, 7, 3, 21, 22) which in turn, will affect leaf gas exchange. Comparing leaf structures for polidemics in different habitats suggests that significant differences in internal leaf geometry affect photosynthesis rate. Calculations with the 2DLEAF model demonstrate the effects of the leaf internal structure quantitatively (Fig. 4), and reveal a general relationship between photosynthesis and CAI.

Transpiration rate calculated by 2DLEAF was not significantly affected by the leaf internal structure, or even by the leaf thickness. This is in agreement with our earlier results (18) that water vapor concentration in the intercellular space during steady state transpiration is almost constant and equal to the saturation value at the leaf temperature. It is a little lower only in the substomatal cavity. The gradient of water vapor concentration between the cells surrounding the stomatal cavity and the bulk atmosphere works as the driving force of transpiration and the rate depends primarily on stomatal aperture (Fig. 6), although we can expect the size of the stomatal cavity to have a small effect. Stomatal aperture has a much more pronounced effect on transpiration rate than on photosynthesis (Figs 4 and 6). Simulations in our earlier works (18, 19) showed that even at small stomatal apertures, when water losses were about 13% of the maximum, photosynthesis rate was equal to 90% of its maximum value.

Cowan and Farquhar (4) hypothesized that stomatal aperture regulates photosynthesis and transpiration such that: "the total loss of water during a day is a minimum for a total amount of carbon taken in. This is a basic hypothesis. Stomatal behavior which conforms to it will be called optimal". Our results, along with numerous other observations (1, 2, 7, 22), show that changes in leaf

anatomy represents an adaptation mechanism that optimizes photosynthesis and transpiration in a changing environment. However, the time scales of leaf anatomy changes (weeks) and of stomata regulation (minutes) are quite different. Photosynthesis provides a carbon supply that is essential for the entire life cycle of the plant, but its acquisition, storage, and ultimate use can be integrated over long periods, so its adaptation time scale can be much more than a day. Internal leaf structure is adapted to the environmental conditions during leaf development and growth, thus, carbon uptake is optimized over days through modifications of leaf anatomy. One of the major functions of transpiration is to keep plant temperature below a lethal threshold. Therefore, transpiration should react much faster to weather conditions and its adaptation time scale has to be very short, i.e., minutes.

Changes in leaf anatomy in changing environments imply that care should be taken when using one-dimensional leaf gas exchange models, especially for predicting consequences of global climate change. Parameters of these models determined for current conditions may not be valid for leaves adapted to different conditions. The results of this work highlight the need for studies of changes in leaf anatomy induced by environmental changes. Data of this type are very scarce, but they are as important as data on the effect of $[CO_2]$ on stomatal density (10, 28).

ACKNOWLEDGEMENTS

We thank Christian Korner for helpful and encouraging discussion. We appreciate the critical reviewing and valuable comments made by James Reynolds, Daryl Moorhead, Paul Kemp, and reviewers of *Biotronics* which improved the manuscript significantly.

REFERENCES

1. Bolhar-Nordenkamp H.R. and Draxler G. (1993) Functional leaf anatomy. Pages 91-128 in D.O. Hall et al. (eds) *Photosynthesis and Production in a Changing Environment: A Field and Laboratory Manual* eds. Chapman & Hall, London.
2. Clements E.S. (1905) The relation of leaf structure to physical factors. *Trans. Am. Microsc. Soc.* **25**, 19-102.
3. Cormack R.G.H. and Gorham A.L. (1953) Effects of exposure to direct sunlight upon the development of leaf structure of two deciduous shrub species. *Can. J. Bot.* **31**, 537-541.
4. Cowan I.R. and Farquhar G.D. (1977) Stomatal function in relation to leaf metabolism and environment. Pages 471-505 in *Integration of Activity in the Higher Plant., Symposia of the Society for Experimental Biology*, Vol. 31, Cambridge University Press, Cambridge, London.
5. Dengler N.G., Dengler R.E., Donnelly P.M., and Hattersley P.W. (1994) Quantitative leaf anatomy of C_3 and C_4 grasses (Poaceae): Bundle sheath and mesophyll surface area relationships. *Ann. Bot.* **73**, 241-255.
6. Farquhar G.D., von Caemmerer S., and Berry J.A. (1980) A biochemical model of photosynthetic CO_2 assimilation in leaves of C_3 species. *Planta* **149**, 78-90.
7. Hanson H.C. (1917) Leaf structure as related to environment. *Am. J. Bot.* **4**, 533-560.

8. Harley P.C. and Tenhunen J.D. (1991) Modeling the photosynthetic response of C₃ leaves to environmental factors. Pages 17–39 in *Modeling Crop Photosynthesis—from Biochemistry to Canopy*. CSSA, Madison.
9. Jones H.G. (1992) *Plants and Microclimate: A Quantitative Approach to Environmental Plant Physiology*. Second Edition. Cambridge University Press, Cambridge, UK, p.428
10. Korner Ch. (1988) Does global increase of CO₂ alter stomatal density? *Flora* **181**, 253–257.
11. Kubinova L. (1991) Stomata and mesophyll characteristics of barley leaf as affected by light: Stereological analysis. *J. Exp. Bot.* **42**, 995–1001.
12. Long S.P. and Hallgren J.-E. (1993) *Measurement of CO₂ assimilation by plants in the field and the laboratory*. Pages 129–167 in D.O. Hall *et al.* (eds.) *Photosynthesis and Production in Changing Environment. A Field and Laboratory Manual*. Chapman and Hall, London etc.
13. Madsen E. (1973) Effect of CO₂-concentration on the morphological, histological, and cytological changes in tomato plants. *Acta Agric. Scand.* **23**, 241–246.
14. Mooney H.A., Drake B.G., Luxmore R.J., Oechel W.C., and Pitelka L.E. (1991) Predicting ecosystem responses to elevated CO₂ concentrations. What has been learned from laboratory experiment on plant physiology and field observations? *Bio Sci.* **41**, 96–104.
15. Morison J.I.L and Gifford R.M. (1984) Plant growth and water use with limited water supply in high CO₂ concentration. I. Leaf area, water use, and transpiration. *Austr. J. Plant Physiol.* **11**, 361–374.
16. Moskaleva G.I. and Sinel'nikova V.N. (1977) Characteristics of an anatomical structure of a tomato leaf as affected by cultivation under conditions of salinization. *Bulletin Vsesojusnogo Instituta Rastenievodstva, Leningrad* **47**, 6–11 (in Russian).
17. Nobel P.S. (1991) *Physicochemical and Environmental Plant Physiology*. Acad. Press, San Diego.
18. Pachepsky L.B., Haskett J.D., and Acock B. (1995) A two-dimensional model of leaf gas exchange with special reference to leaf anatomy. *J. Biogeograph.* **22**, 1101–1106.
19. Pachepsky L.B. and Acock B. (1996) 2DLEAF— A model of leaf gas exchange: Development, validation, and ecological application. *Ecol. Model.* **93**, 1–18.
20. Pachepsky L.B., Acock B., Hoffman-Benning Willmitzer L., and Fisahn J. (1997) Estimation of the anatomical, stomatal and biochemical components of differences in photosynthesis and transpiration of wild-type and transgenic (expressing yeast-derived invertase targeted to the vacuole) tobacco leaves. *Plant, Cell, and Environ.* **20**, 1070–1078.
21. Rogers H.H., Bingham G.E., Cure J.D., Heck W.W., Heagle A.S., Israel D.W., Smith J.M., Surano K.A., and Thomas J.F. (1980) *Field Studies of Plant Responses to Elevated Carbon Dioxide Levels*, p. 113. USDA, ARS, North Carolina State University, Raleigh, NC.
22. Salisbury F.B. and Ross C.W. (1991) *Plant Physiol.* 4th Ed. Wadsworth Publishing Company, Belmont. p. 682.
23. Sims D.A. and Pearcy R.W. (1992) Response of leaf anatomy and photosynthetic capacity in *Alocasia macrorrhiza* (Araceae) to a transfer from low to high light. *Am. J. of Bot.* **79**, 449–455.
24. Syvertsen J.P., Lloyd J., McConchine C., Kriedemann R.E. and Farquhar G.D. (1995) On the relationship between leaf anatomy and CO₂ diffusion through the mesophyll of hypostomatous leaves. *Plant, Cell, and Environ.* **18**, 149–157.
25. Stanghellini C. and Bunce J.A. (1993) Response of photosynthesis and conductance to light, CO₂, temperature, and humidity in tomato plants acclimated to ambient and elevated CO₂. *Photosynthetica* **29**, 487–497.
26. Valle R., Mishoe J.W., Campbell W.J., Jones J.W., and Allen L.H., Jr. (1985) Photosynthetic responses of “Bragg” soybean leaves adapted to different CO₂ environments. *Crop Sci.* **25**, 333–339.

27. Van Volkenburgh E. and Davies W.J. (1977) Leaf anatomy and water relations of cotton plants grown in controlled environments and in the field. *Crop Sci.* **17**, 353-359.
28. Woodward F.I. (1987) Stomatal numbers are sensitive to increases in CO₂ from preindustrial levels. *Nature* **327**, 617-618.